

RAMAN CHARACTERIZATION OF $\text{CuCr}_{2-x}\text{Sn}_x\text{S}_4$ SPINELS

P. VALENCIA-GÁLVEZ^a, O. PEÑA^b, S. MORIS^{*c}, P. BARAHONA^{*d}

^aFacultad de Ciencias, Departamento de Química, Universidad de Chile, Las Palmeras 3425, Santiago, 7800003 Chile

^bInstitut des Sciences Chimiques de Rennes, UMR 6226, Université de Rennes 1, Rennes, France

^cVicerrectoría de Investigación y postgrado, Universidad Católica del Maule, Avenida San Miguel 3605, Talca 3480112, Chile

^dFacultad de Ciencias Básicas, Universidad Católica del Maule, Avenida San Miguel 3605, Talca 3480112, Chile

ABSTRACT

Polycrystalline thiospinels $\text{CuCr}_{2-x}\text{Sn}_x\text{S}_4$ ($x = 0.4, 0.8, 1.0$ and 1.4) were synthesized via conventional solid-state reaction. The samples were characterized by powder X-ray diffraction (XRD), energy-dispersive X-ray analysis (SEM-EDS) and Raman spectroscopy. All the samples were indexed in the space group $Fd\bar{3}m$. The Raman spectra confirmed the structure of normal spinel type with five characteristic signals for the active modes in Raman. Magnetic measurements, performed for the phases with $x = 0.8$ and 1.0 , showed irreversible antiferromagnetism with dominant ferromagnetism and spin glass behavior.

Keywords: thiospinels, Raman spectroscopy, magnetic measurements.

1. INTRODUCTION

Compounds with formula AB_2X_4 correspond to cubic-spinel structure (space group $Fd\bar{3}m$) with $X = \text{O}, \text{S}, \text{Se}$; $A = \text{Cu}, \text{Ag}, \text{Mg}$; $B = \text{Cr}, \text{Al}, \text{In}, \text{Ti}, \text{Sn}$ [1], [2]. The normal spinel structure presents B cations in octahedral sites (16d) and A cations in tetrahedral sites (8a). The unit cell contains X anions (bonded to one A and three B cations) in a cubic close-packing arrangement (32e site).

CuCr_2X_4 spinel-type exhibit interesting magnetic, electrical and optical properties. These properties can be modified by substituting metal ions at tetrahedral (A) [3], [4] or octahedral positions (B) by other ions. The substitution of Cr by M to form $\text{CuCr}_{2-x}\text{Sn}_x\text{S}_4$ can modify the magnetic properties from ferromagnetism to spin-glass behavior. This has been observed in CuCrTiS_4 [2] and CuCrZrS_4 [5] spinels, which present a marked effect on their magnetic properties due to the presence of the substituent cation in position B. These types of spinels have gained attention in recent years since they exhibit a rich variety of physical phenomena, including colossal magnetoresistance, giant red-shift of the absorption edge, magnetic field-induced structural transformation, multi-ferroicity, spin and orbital frustration among other properties [6].

In these compounds, Cr^{3+} is octahedrally surrounded by X ions ($X = \text{chalcogen}$) with a half-filled t_{2g} ground state ($S = 3/2$), resulting in no charge and no orbital degrees of freedom. Thus, the magnetic properties originate predominantly from exchange and superexchange interactions between Cr^{3+} ions [7], [8].

The magnetic properties of $\text{CuCr}_{2-x}\text{Sn}_x\text{S}_4$, with $x = 1.0$, have been previously studied [3], [9], presenting an antiferromagnetic and spin-glass behaviors. Raman spectroscopy has been reported only in selenium compounds $\text{CuCr}_{2-x}\text{M}_x\text{Se}_4$ presenting a variation in the frequency of the main vibrational modes, due to the disorder generated by the chemical substitution of Cr by M ($M = \text{Sn}$ and Zr) [10]. It has also been observed that the displacements that affect the distance Cr-X ($X = \text{S}, \text{Se}$) influence the magnetic behavior of this type of compounds [11]. Nevertheless, Raman characterization of CuCrSnS_4 phase has not been yet documented in particular optical changes caused by the replacement of Cr by Sn.

The present work describes the solid-state synthesis of $\text{CuCr}_{2-x}\text{Sn}_x\text{S}_4$ ($x = 0.4, 0.8, 1.0$ and 1.4) phases, powder X-ray diffraction, magnetic measurements and Raman characterization in order to determine the influence of chemical substitution on the structure and magnetic properties of these compounds.

2. MATERIAL AND METHODS

2.1. Synthesis

$\text{CuCr}_{2-x}\text{Sn}_x\text{S}_4$ compounds were prepared directly by combining high-purity elemental powders (99.99%, Aldrich) in stoichiometric amounts. All manipulations were carried out under argon atmosphere. The reaction mixtures were sealed in evacuated quartz ampoules and placed in a programmable furnace. The ampoules were then slowly heated at a rate of $1^\circ\text{C}/\text{min}$, from room temperature until 850°C , and held for 6 days. Then, ampoules were slowly cooled, opened, homogenized, resealed and heated again to the same temperature of 850°C and maintained for 10 days. Finally, they were again slowly cooled to

room temperature at a rate of $1^\circ\text{C}/\text{min}$, ready for their characterization.

2.2. Powder X-ray Diffraction

Powder X-ray diffraction (PXRD) patterns were collected at room temperature on a Bruker D8 Advance diffractometer equipped with a $\text{Cu K}\alpha$ radiation source ($K\alpha = 1.5406 \text{ \AA}$); samples were scanned in the range $5^\circ < 2\theta < 80^\circ$.

2.3. SEM-EDS analysis

The chemical compositions of samples were determined by scanning electron microscopy with the aid of energy-dispersive X-ray analysis (SEM-EDS) using a JEOL 5400 system equipped with an Oxford Link ISIS microanalyzer. The working distance was 35 mm and the accelerating voltage was set to 22.5 kV. Samples were mounted into a double-sided carbon tape, which was adhered to an aluminum specimen holder. EDS data were collected for 60 s.

2.4. Raman spectroscopy

The Raman scattering measurements of $\text{CuCr}_{2-x}\text{Sn}_x\text{S}_4$ were made using a RM1000 Renishaw micro-Raman spectrometer with detectors CCD (Charge-Coupled Device) in combination with a Leica LM/PM microscope using excitation of 532 nm wavelength. The spectrometer was calibrated using a reference single crystal Si sample (Raman peak at 520.7 cm^{-1}). The spectra data was collected at room temperature in back scattering configuration in the spectral range $100 - 450 \text{ cm}^{-1}$, with a laser spot on the sample of about $\sim 1 \mu\text{m}$ and a laser power $\sim 2\text{mW}$.

2.5. Magnetic measurements

Magnetic measurements were performed on pelletized powder samples using a Quantum Design MPMS XL5 SQUID susceptometer. The magnetic nature of the material was determined using ZFC/FC (zero-field-cooled/field-cooled) cycles at low fields (typically 500 Oe).

3. RESULTS AND DISCUSSION

3.1 Powder X-ray diffraction and SEM-EDS

The XRD patterns were fully indexed in the space group $Fd\bar{3}m$ ($N^\circ 227$), indicating that $\text{CuCr}_{2-x}\text{Sn}_x\text{S}_4$ compounds present spinel-type structures. The experimental XRD patterns were compared with the simulated XRD patterns derived from a single-crystal XRD data. Experimental XRD patterns for $\text{CuCr}_{2-x}\text{Sn}_x\text{S}_4$ thiospinels are shown in Fig. 1. For these compounds, the cell parameter " a " increased gradually as chromium was replaced by tin (Table 1), obeying Vegard's law. This can be explained by the higher ionic radii of Sn^{4+} compared to Cr^{3+} ions. The octahedral ionic radii of Sn^{4+} and Cr^{3+} cations published by Shannon are 0.69 \AA and 0.615 \AA , respectively (for a high-spin configuration) [12]. This shows that the increase in ionic radius explains the increase in the size of the unit cell. Chemical compositions of powder samples were examined using EDS analysis (Fig. 2).

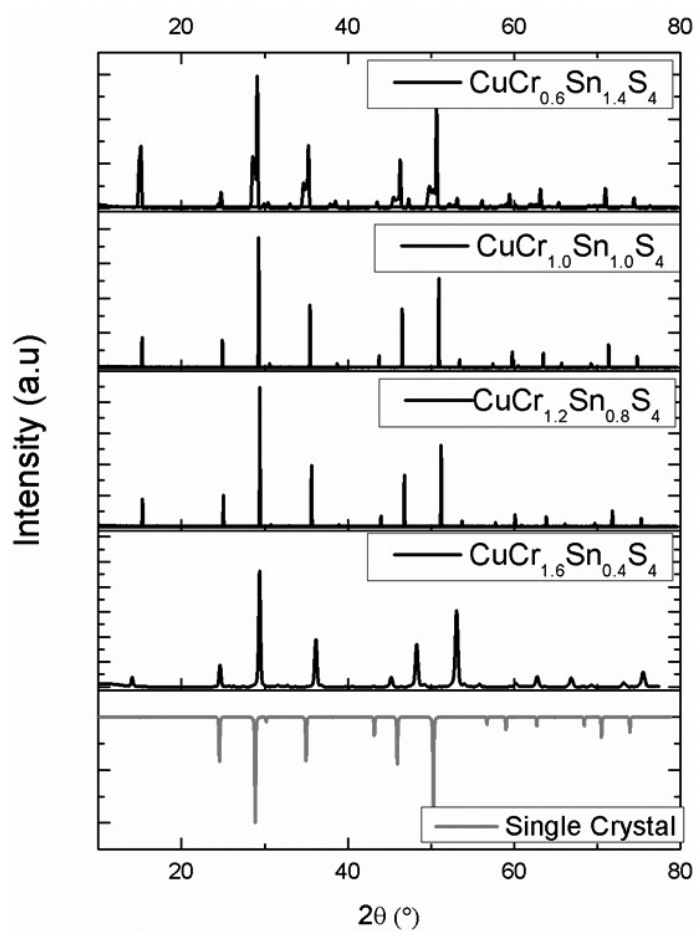


Fig. 1. Experimental X-ray powder diffraction patterns for $\text{CuCr}_{2x}\text{Sn}_{1-x}\text{S}_4$ compared with simulated X-ray pattern of $\text{CuCr}_{1.2}\text{Sn}_{0.8}\text{S}_4$ single crystal [13].

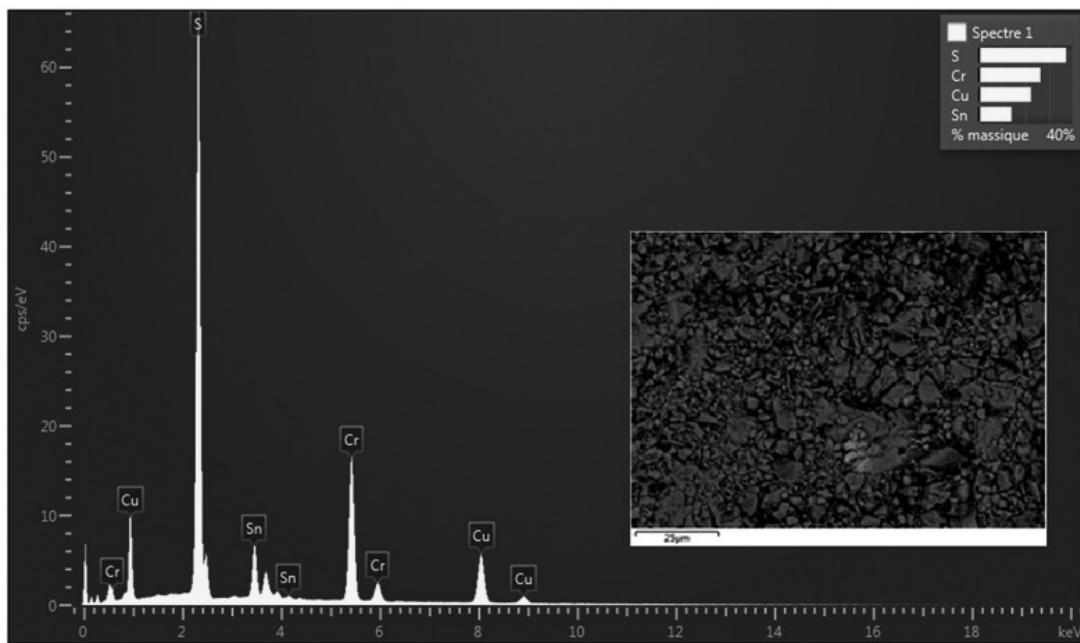


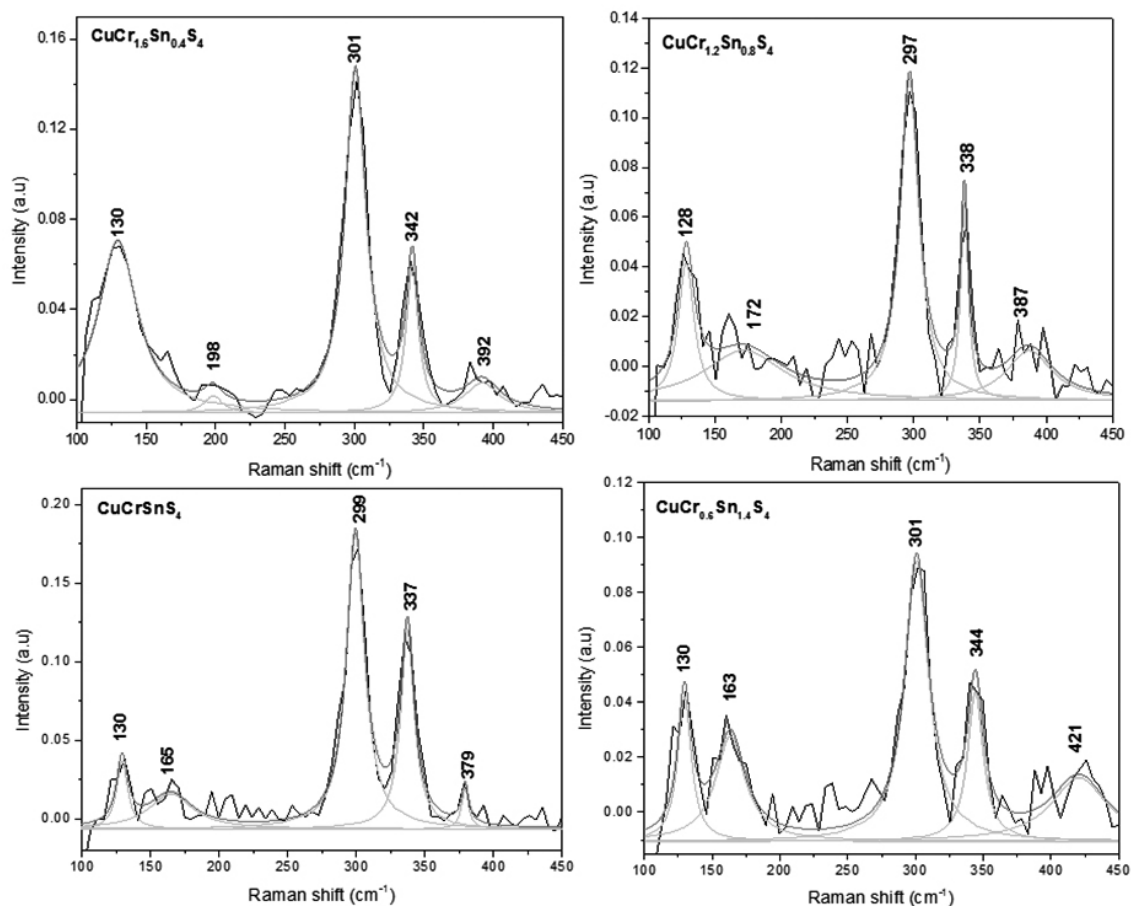
Fig.2. Scanning electron microscopy (SEM) micrograph of $\text{CuCr}_{1.6}\text{Sn}_{0.4}\text{S}_4$ (insert) and an example of EDS spectral analysis.

Table 1. Lattice parameters (XRD powder data) and chemical analytical data for thio-spinel compounds.

Compound	Cell parameter a (Å)	Compositions from EDS analyses
$\text{CuCr}_{1.6}\text{Sn}_{0.4}\text{S}_4$	9.962	$\text{Cu}_{1.13}\text{Cr}_{1.63}\text{Sn}_{0.38}\text{S}_{3.75}$
$\text{CuCr}_{1.2}\text{Sn}_{0.8}\text{S}_4$	10.12	$\text{Cu}_{1.00}\text{Cr}_{1.22}\text{Sn}_{0.80}\text{S}_{3.95}$
$\text{CuCr}_{1.0}\text{Sn}_{1.0}\text{S}_4$	10.17	$\text{Cu}_{1.11}\text{Cr}_{1.08}\text{Sn}_{0.97}\text{S}_{3.87}$
$\text{CuCr}_{0.6}\text{Sn}_{1.4}\text{S}_4$	10.22	$\text{Cu}_{1.04}\text{Cr}_{0.54}\text{Sn}_{1.44}\text{S}_{3.85}$

3.2 Raman spectroscopy

Brüesch and D'Ambrogio [14] have performed a detailed Raman analysis for CdCr_2X_4 (X = S, Se). Through group theory, the authors, assigned the signals to the corresponding symmetrical modes, characteristic of the spinel crystal structure with spatial group. The irreducible representation is $\Gamma = A_{1g} + E_g + F_{2g} + 3F_{2g} + 2A_{2u} + 2E_u + 5F_{1u} + 2F_{2u}$, where the modes A_{1g} , E_g and the three F_{2g} are active in Raman. The Raman spectra for the four studied compositions $\text{CuCr}_{2-x}\text{Sn}_x\text{S}_4$ ($0.4 \leq x \leq 1.4$) were measured under light excitation with wavelength of 532 nm, in the spectral region between 100 and 450 cm^{-1} and adjusted by means of Lorentzian functions (Fig. 3).

**Fig. 3.** Raman Spectra of $\text{CuCr}_{2-x}\text{Sn}_x\text{S}_4$ ($0.4 \leq x \leq 1.4$) powder samples.

The spectra were characterized by five signals, showing a good similarity with the normal spinels ACr_2S_4 (A = Cd, Hg) [11], [14]-[18]. Table 2 presents a summary of the peaks position and the corresponding symmetry.

Table 2. Frequency (in cm^{-1}) and proposed assignment modes of Raman peaks for solid solutions $\text{CuCr}_{2-x}\text{Sn}_x\text{S}_4$.

Mode	$\text{CuCr}_{2-x}\text{Sn}_x\text{S}_4$			
	x = 0.4	x = 0.8	x = 1.0	x = 1.4
$F_{2g}(1)$	130	128	130	130
E_g	198	172	165	163
$F_{2g}(2)$	301	297	299	301
$F_{2g}(3)$	342	338	337	344
A_{1g}	392	387	379	421

Specifically, the signals about 130 cm^{-1} , 300 cm^{-1} and near to 400 cm^{-1}

reflect the vibrations in the thiospinels tetrahedron, where the mode $F_{2g}(1)$ at 130 cm^{-1} , is attributed to bending of the CuS_4 unit, while the mode $F_{2g}(2)$ at 300 cm^{-1} corresponds to asymmetric stretching of the tetrahedron. For its part, the A_{1g} mode at ~ 400 cm^{-1} corresponds to symmetric stretching of the Cu-S bond in the CuS_4 unit [14], [15], [18]. Although, the latest signal reflects a vibration of the tetrahedron, we observe the influence of the substitution at the octahedral site (16d), which is randomly occupied by the chromium and tin cations. The signal A_{1g} shows a widening and displacement toward higher frequencies, particularly important in the $\text{CuCr}_{0.6}\text{Sn}_{1.4}\text{S}_4$ phase, which correspond to an increase in the force constant of the Cu-S bond in the CuS_4 unit. We suggest that, as the content of the Sn^{4+} cation ionic radius of 0.69 Å [12] increases, it induces an increase in the stress within the tetrahedron.

On the other hand, the E_g and $F_{2g}(3)$ modes have been assigned to the symmetric and antisymmetric twisting motion of the cation on the Cr/Sn-S link of the BS_6 unit [14], [15]. Particularly, the signal corresponding to the E_g mode undergoes a shift toward low energies (Table 2), showing the influence of the substitution of chromium by tin. This result is consistent with the tin content in the samples, since the atomic weight of Sn is greater than the chromium one, leading to red shift of the signals.

This set of results allows us to propose the modes A_{1g} and E_g as those responsible to qualitatively prove the presence of tin in the phases, confirming new chemical interactions which explain changes in the force constants of the structure.

3.3 Magnetic measurements

The zero-field-cooled (ZFC)/field-cooled (FC) magnetization cycles for $\text{CuCr}_{2-x}\text{Sn}_x\text{S}_4$ ($x = 0.8$ and 1.0) were performed under a magnetic field of 500 Oe (Fig. 4 and 5). The insets show the inverse susceptibility in the paramagnetic regime. The inverse susceptibility, $1/\chi$, was fitted with a classical Curie-Weiss relation, $\chi = C/(T-\theta)$, in a temperature range that varied depending on the compound.

In both samples, an antiferromagnetic behavior is observed with a Néel temperature T_N equal to 17.8 K and 24.8 K for $\text{CuCr}_{1.0}\text{Sn}_{1.0}\text{S}_4$ and $\text{CuCr}_{1.2}\text{Sn}_{0.8}\text{S}_4$ respectively. However, the sample with $x = 0.8$ shows a positive value of θ (+84.2 K, Table 3) which indicates a dominant ferromagnetic character of the exchange interactions (Fig. 5). Both samples ($x = 0.8$ and 1.0) present an irreversible behavior below the transition temperature that could be associated to a spin glass state. This behavior can be correlated to the increase of the cell parameter "a" (Table 1) that favors an antiferromagnetic interaction when Sn content increased, changing the orientation of the localized magnetic moment and causing that the spin glass state appears. A similar result has been reported in CuCrZrS_4 [5] and $\text{CuCr}_{2-x}\text{Sn}_x\text{Se}_4$ [10] compounds.

The observed magnetic moments for $\text{CuCr}_{1.0}\text{Sn}_{1.0}\text{S}_4$ ($\mu_{\text{eff}} = 3.79$ MB) and $\text{CuCr}_{1.2}\text{Sn}_{0.8}\text{S}_4$ ($\mu_{\text{eff}} = 3.82$ MB) are close to the moments expected for high-spin states $\text{Cu}^{1+}[\text{Cr}_{1-x}^{3+}\text{Cr}_{(1-x)}^{4+}]\text{Sn}_x^{4+}\text{S}_4$ ($\mu_{\text{theo}} = 4.07$ MB and $\mu_{\text{theo}} = 3.87$ MB for $x=1.0$ and 0.8) [19].

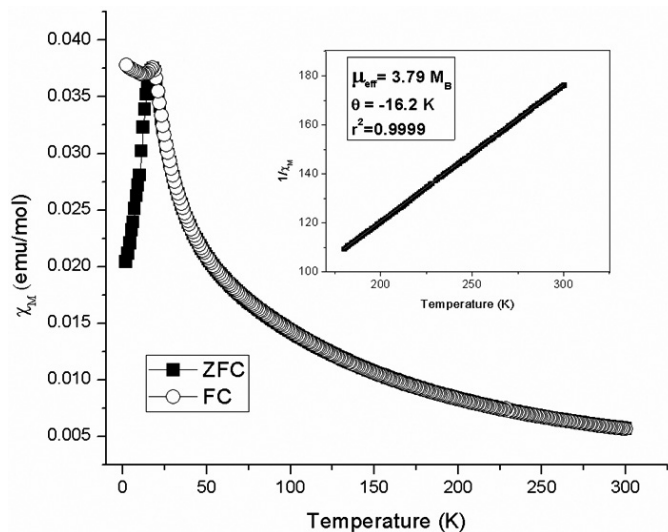


Fig. 4. ZFC/FC magnetization cycle measured at $H_{\text{app}} = 500$ Oe for a powder sample of $\text{CuCr}_{1.0}\text{Sn}_{1.0}\text{S}_4$. The insert shows the $1/\chi$ -versus-temperature behavior fitted by a Curie-Weiss law.

Table 3. Magnetic parameters for thiospinels compounds.

Compound	T_N (K)	μ_{eff} (MB)	θ (K)
$\text{CuCr}_{1.0}\text{Sn}_{1.0}\text{S}_4$	17.8	3.79	-16.2
$\text{CuCr}_{1.2}\text{Sn}_{0.8}\text{S}_4$	24.8	3.82	+84.2

CONCLUSIONS

Powder samples of $\text{CuCr}_{2-x}\text{Sn}_x\text{S}_4$ ($x = 0.4, 0.8, 1.0$ and 1.4) were obtained by conventional solid-state synthesis. The X-ray diffraction of the powder samples indicated that all phases crystallized in cubic spinel-type structures.

From Raman spectroscopy, we identified five active Raman signals characteristic of thiospinels. The broadening and displacement of signals assigned to E_g and A_{1g} modes were attributed to new chemical interactions caused by the substitution of chromium by tin at the B site. Particularly, the E_g mode shows a significant shift to low energies, directly related to the increase content of

tin substitution in the lattice. Instead, for A_{1g} mode, we propose a higher stress for the tetrahedron CuS_4 caused by the substitution of Cr by Sn that possess a greater ionic radius.

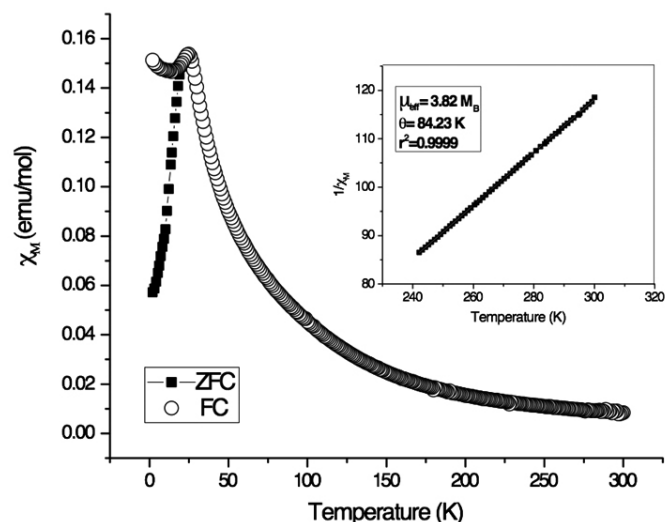


Fig. 5. ZFC/FC magnetization cycle measured at $H_{\text{app}} = 500$ Oe for a powder sample of $\text{CuCr}_{1.2}\text{Sn}_{0.8}\text{S}_4$. The insert shows the $1/\chi$ -versus-temperature behavior fitted by a Curie-Weiss law.

The magnetic susceptibility measurements performed for samples $x=1.0$ and 0.8 showed an antiferromagnetic behavior. The substitution of Cr by Sn simultaneously weakens the ferromagnetic nearest neighbor exchange between Cr ions and promotes the remaining antiferromagnetic next-nearest neighbor interactions with appearance of a spin glass behavior.

ACKNOWLEDGMENTS

This work was supported by FONDECYT 1161020 and the Chilean-French International Associated Laboratory for "Multifunctional Molecules and Materials" (LIAM3-CNRS N°1027).

REFERENCES

- [1] J. Ruiz-Fuertes, D. Errandonea, F.J. Manjón, D. Martínez-García, A. Segura, V. V. Ursaki, I.M. Tiginyanu, High-pressure effects on the optical-absorption edge of CdIn_2S_4 , MgIn_2S_4 , and MnIn_2S_4 thiospinels, J. Appl. Phys. 103 (2008) 1–5. doi:10.1063/1.2887992.
- [2] F. Kariya, S. Ebusu, S. Nagata, Evolution from a ferromagnetic to a spin-glass regime in the spinel-type $\text{Cu}(\text{Cr}_{1-x}\text{Ti}_x)_2\text{S}_4$, J. Solid State Chem. 182 (2009) 608–616. doi:10.1016/j.jssc.2008.12.008.
- [3] T. Ishikawa, S. Ebusu, S. Nagata, Spin-glass and novel magnetic behavior in the spinel-type $\text{Cu}_{1-x}\text{Ag}_x\text{CrSnS}_4$, Phys. B Condens. Matter. 405 (2010) 1881–1889. doi:10.1016/j.physb.2010.01.067.
- [4] R. Plumier, M. Sougi, Magnetic ordering in the normal spinel $\text{Cu}_{0.5}\text{In}_{0.5}\text{Cr}_2\text{Se}_4$, Solid State Comm. 69 (1989) 341–345.
- [5] Y. Iijima, Y. Kamei, N. Kobayashi, J. Awaka, T. Iwasa, S. Ebusu, S. Chikazawa, S. Nagata, A new ferromagnetic thiospinel CuCrZrS_4 with re-entrant spin-glass behaviour, Philos. Mag. 83 (2003) 2521–2530. doi:10.1080/0141861031000109609.
- [6] V.A. Fedorov, Y.A. Kesler, E.G. Zhukov, Magnetic semiconducting chalcogenide spinels: Preparation and physical chemistry, Inorg. Mater. 39 (2003) S68–S88. doi:10.1023/B:INMA.0000008887.85985.6b.
- [7] F.K. Lotgering, Ferromagnetism in spinels: CuCr_2S_4 and CuCr_2Se_4 , Solid State Commun. 2 (1964) 55–56. doi: 10.1016/0038-1098(64)90573-3.
- [8] C. Pang, L. Gao, A. Chaturvedi, N. Bao, K. Yanagisawa, L. Shen, A. Gupta, High-temperature solvothermal synthesis and magnetic properties of nearly monodisperse CdCr_2S_4 nanocrystals, J. Mater. Chem. C. 3 (2015) 12077–12082. doi:10.1039/C5TC02727F.
- [9] P. Colombet, J. Soubeyroux, M. Danot, Spin correlations in the $\text{Cu}_{2x}\text{Cr}_{2-2x}\text{Sn}_{2-2x}\text{S}_4$ spinel spin glasses, J. Magn. Mater. 51 (1985) 257–264.
- [10] C. Pinto, A. Galdámez, P. Barahona, S. Moris, O. Peña, Crystal struc-

- ture, Raman scattering and magnetic properties of $\text{CuCr}_{2-x}\text{Zr}_x\text{Se}_4$ and $\text{CuCr}_{2-x}\text{Sn}_x\text{Se}_4$ selenospinel, *J. Magn. Magn. Mater.* 456 (2018) 160–166. doi:10.1016/j.jmmm.2018.02.023.
- [11] V. Gnezdilov, P. Lemmens, Y.G. Pashkevich, C. Payen, K.Y. Choi, J. Hemberger, A. Loidl, V. Tsurkan, Phonon anomalies and possible local lattice distortions in giant magnetocapacitive CdCr_2S_4 , *Phys. Rev. B* 84 (2011) 1–6. doi:10.1103/PhysRevB.84.045106.
- [12] R.D. Shannon, Revised effective ionic radii and systematic studies of interatomic distances in halides and chalcogenides, *Acta Crystallogr. Sect. A.* 32 (1976) 751–767. doi:10.1107/S0567739476001551.
- [13] M. Tremblat, P. Colombet, J. Rouxel, M. Danot, Les system pseudobinaires $\text{CuCrS}_2\text{-MeS}_2$ (**Me = Ti, Sn**): $\text{Cu}_y\text{Cr}_y\text{M}_{2-y}\text{S}_4$ ($\text{Cu}_x\text{Cr}_x\text{M}_{1-x}\text{S}_2$) Spinel. *Rev. Chim. Min.* 17 (1980) 183-191.
- [14] F. Brüesch, P. D'Ambrogio, Lattice Dynamics and Magnetic Ordering in the chalcogenide spinels CdCr_2S_4 and CdCr_2Se_4 , *Phys. Stat. Sol.* 50 (1972) 513–526.
- [15] N. Koshizuka, S. Ushioda, T. Tsushima, Resonance Raman scattering in CdCr_2S_4 . Magnetic-circular-polarization properties, *Phys. Rev. B.* 21 (1980) 1316–1322.
- [16] C.J. Fennie, K.M. Rabe, Polar phonons and intrinsic dielectric response of the ferromagnetic insulating spinel CdCr_2S_4 from first principles, *Phys. Rev.* 72 (2005) 1–5. doi:10.1103/PhysRevB.72.214123.
- [17] I. Efthimiopoulos, A. Yaresko, V. Tsurkan, J. Deisenhofer, A. Loidl, C. Park, Y. Wang, Multiple pressure-induced transitions in HgCr_2S_4 , *Appl. Phys. Lett.* 103 (2013) 1–6. doi:10.1063/1.4830225.
- [18] V.G. Ivanov, M.N. Iliev, Y.H.A. Wang, A. Gupta, Ferromagnetic spinel $\text{Cu-Cr}_2\text{Se}_4$ studied by Raman spectroscopy and lattice dynamics calculations, *Phys. Rev.* 81 (2010) 1–5. doi:10.1103/PhysRevB.81.224302.
- [19] M.M. Ballal, C. Mande, X-ray spectroscopic study of the valency of copper in the spinels CuCr_2X_4 ($\text{X} = \text{O}, \text{S}, \text{Se}, \text{Te}$), *Solid State Commun.* 19 (1976) 325–327. doi:10.1016/0038-1098(76)91343-0.